Title
ENERGY-DISPERSIVE X-RAY FLUORESCENCE (EDXRF) WHOLE ROCK ANALYSIS OF MAJOR, MINOR ANDTRACE ELEMENTS FOR SANTIAGO PEAK VOLCANIC ROCKS(SPV), LUSARDI FORMATION LOCALITY, NORTHERN SAN DIEGO COUNTY, CALIFORNIA

Author
Shackley, M. Steven

Publication Date
2019-11-27

GEOARCHAEOLOGICAL XRF LAB
A GREEN SOLAR FACILITY

GEOARCHAEOLOGICAL X-RAY FLUORESCENCE SPECTROMETRY LABORATORY
8100 Wyoming Blvd., Ste M4-158 Albuquerque, NM 87113
USA

ENERGY-DISPERSIVE X-RAY FLUORESCENCE (EDXRF) WHOLE ROCK ANALYSIS OF MAJOR, MINOR AND TRACE ELEMENTS FOR SANTIAGO PEAK VOLCANIC ROCKS (SPV), LUSARDI FORMATION LOCALITY, NORTHERN SAN DIEGO COUNTY, CALIFORNIA

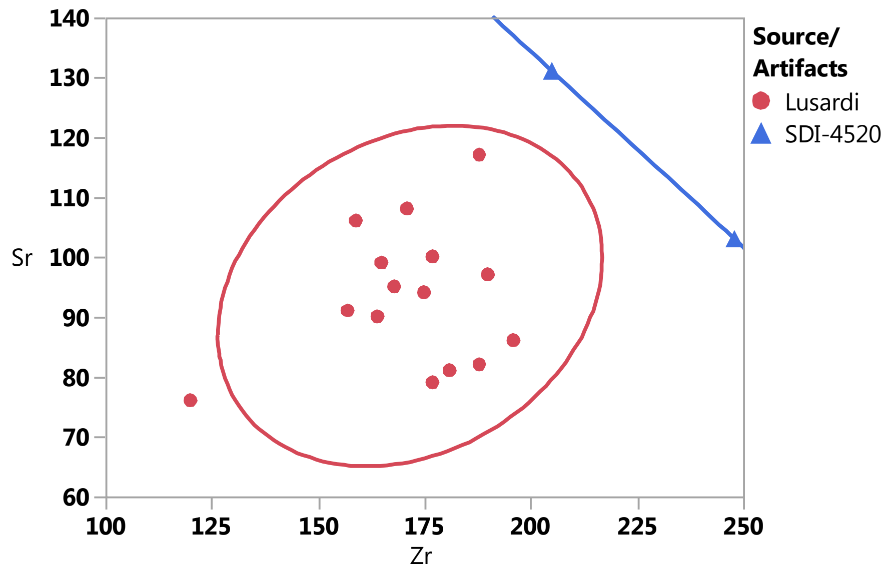

DRAFT

by

M. Steven Shackley, Ph.D., Director
Geoarchaeological XRF Laboratory
Albuquerque, New Mexico

Report Prepared for

Andrew Pigniolo
Laguna Mountain Environmental, Inc.
San Diego, California

27 November 2019

INTRODUCTION

The analysis here of 16 source samples from Santiago Peak Volcanics, Lusardi Formation rock samples indicates some variability in composition, but mainly high silica rhyolites. The composition, however, appears distinctive from the Santiago Peak Volcanics in southern San Diego County in the Middle Sweetwater River area, called colloquially the Dictionary Hill/Mount Miguel Formation of aphyric fine-grained black and green high silica rhyolites (see discussion; Herzig and Kimbrough 2014; Shackley 2017; Tanaka et al. 1984). At this first approximation it appears that there is some variability in the composition of the various Santiago Peak volcanic rock localities such that some elemental discrimination may be possible. Santiago Peak was used so commonly for chipped stone tool production, particularly projectile points in western San Diego County that there is a promise that more intensive source provenance studies in regional prehistoric contexts would be fruitful (see Pigniolo 1996; Shackley 2017).

LABORATORY SAMPLING, ANALYSIS AND INSTRUMENTATION

All archaeological samples are analyzed whole. The results presented here are quantitative in that they are derived from "filtered" intensity values ratioed to the appropriate x-ray continuum regions through a least squares fitting formula rather than plotting the proportions of the net intensities in a ternary system (McCarthy and Schamber 1981; Schamber 1977). Or more essentially, these data through the analysis of international rock standards, allow for inter-instrument comparison with a predictable degree of certainty (Hampel 1984; Shackley 2011).

All analyses for this study were conducted on a ThermoScientific *Quant'X* EDXRF spectrometer, located at the Geoarchaeological XRF Laboratory, Albuquerque, New Mexico. It is equipped with a thermoelectrically Peltier cooled solid-state Si(Li) X-ray detector, with a 50 kV, 50 W, ultra-high-flux end window bremsstrahlung, Rh target X-ray tube and a 76 µm (3 mil) beryllium (Be) window (air cooled), that runs on a power supply operating from 4-50 kV/0.02-

1.0 mA at 0.02 increments. The spectrometer is equipped with a 200 l min^{-1} Edwards vacuum pump, allowing for the analysis of lower-atomic-weight elements between sodium (Na) and titanium (Ti). Data acquisition is accomplished with a pulse processor and an analogue-to-digital converter. Elemental composition is identified with digital filter background removal, least squares empirical peak deconvolution, gross peak intensities and net peak intensities above background.

Trace Element Analysis

The analysis for mid Zb condition elements Ti-Nb, Pb, Th, the x-ray tube is operated at 30 kV, using a 0.05 mm (medium) Pd primary beam filter in an air path at 100 seconds livetime to generate x-ray intensity $K\alpha_1$-line data for elements titanium (Ti), manganese (Mn), iron (as $Fe_2O_3^T$), cobalt (Co), nickel (Ni), copper, (Cu), zinc, (Zn), gallium (Ga), rubidium (Rb), strontium (Sr), yttrium (Y), zirconium (Zr), niobium (Nb), lead (Pb), and thorium (Th). Not all these elements are reported since their values in many volcanic rocks are very low. Trace element intensities were converted to concentration estimates by employing a linear calibration line ratioed to the Compton scatter established for each element from the analysis of international rock standards certified by the National Institute of Standards and Technology (NIST), the US. Geological Survey (USGS), Canadian Centre for Mineral and Energy Technology, and the Centre de Recherches Pétrographiques et Géochimiques in France (Govindaraju 1994). Line fitting is linear (XML) for all elements. When barium (Ba) is analyzed in the High Zb condition, the Rh tube is operated at 50 kV and up to 1.0 mA, ratioed to the bremsstrahlung region (see Davis 2011; Shackley 2011). Further details concerning the petrological choice of these elements in Southwest obsidians is available in Shackley (1988, 1995, 2005; also Mahood and Stimac 1991; and Hughes and Smith 1993). Nineteen specific pressed powder standards are used for the best fit regression calibration for elements Ti-Nb, Pb, Th, and Ba, and include G-2 (basalt), AGV-2 (andesite), GSP-2 (granodiorite), SY-2 (syenite), BHVO-2 (hawaiite), STM-1 (syenite), QLO-1 (quartz latite), RGM-1 (obsidian), W-2 (diabase), BIR-1 (basalt), SDC-1 (mica schist), TLM-1 (tonalite), SCO-1 (shale), NOD-A-1 and NOD-P-1 (manganese) all US Geological Survey standards, NIST-278 (obsidian), U.S. National Institute of Standards and Technology, BE-N (basalt) from the Centre de Recherches Pétrographiques et Géochimiques in France, and JR-1 and JR-2 (obsidian) from the Geological Survey of Japan (Govindaraju 1994).

Major and Minor Oxide Analysis

Analysis of the major oxides of Na, Mg, Al, Si, P, K, Ca, Ti, V, Mn, Fe (total), and As is performed under the multiple conditions elucidated below. This whole rock fundamental parameter analysis (theoretical with standards), while not as accurate as destructive analyses (pressed powder and fusion disks) is fairly close to actual, based on the analysis of USGS RGM-1 obsidian or other international standards (see also Shackley 2011). The fundamental parameters (theoretical) method is run under conditions commensurate with the elements of interest and calibrated with 11 USGS standards (RGM-1, rhyolite; AGV-2, andesite; BHVO-1, hawaiite; BIR-1, basalt; G-2, granite; GSP-2, granodiorite; BCR-2, basalt; W-2, diabase; QLO-1, quartz latite; STM-1, syenite), and one Japanese Geological Survey rhyolite standard (JR-1). See Lundblad et al. (2011) for another set of conditions and methods for oxide analyses of basalt.

Conditions Of Fundamental Parameter Analysis[1]:

Low Za (Na, Mg, Al, Si, P)

Voltage	6 kV	Current	Auto[2]
Livetime	100 seconds	Counts Limit	0
Filter	No Filter	Atmosphere	Vacuum
Maximum Energy	10 keV	Count Rate	Low

Mid Zb (K, Ca, Ti, V, Cr, Mn, Fe)

Voltage	32 kV	Current	Auto
Livetime	100 seconds	Counts Limit	0
Filter	Pd (0.06 mm)	Atmosphere	Vacuum
Maximum Energy	40 keV	Count Rate	Medium

High Zb (Sn, Sb, Ba, Ag, Cd)

Voltage	50 kV	Current	Auto
Livetime	100 seconds	Counts Limit	0
Filter	Cu (0.559 mm)	Atmosphere	Vacuum
Maximum Energy	40 keV	Count Rate	High

Low Zb (S, Cl, K, Ca)

Voltage	8 kV	Current	Auto
Livetime	100 seconds	Counts Limit	0
Filter	Cellulose (0.06 mm)	Atmosphere	Vacuum
Maximum Energy	10 keV	Count Rate	Low

[1] Multiple conditions designed to ameliorate peak overlap identified with digital filter background removal, least squares empirical peak deconvolution, gross peak intensities and net peak intensities above background.

[2] Current is set automatically based on the mass absorption coefficient.

Statistical and Graphical Source Analysis

The data from the WinTrace™ software were translated directly into Excel for Windows software for manipulation and on into SPSS, ver. 21 for Windows and/or JMP 12.01 for statistical analyses as appropriate. In order to evaluate these quantitative determinations, machine data were compared to measurements of known standards during each run. RGM-1 a USGS rhyolite (obsidian) standard is analyzed during each sample run of ≤19 to insure instrument calibration/accuracy (Table 1; see Shackley 2011a).

Further information on the laboratory instrumentation and source data can be found at: http://swxrflab.net/anlysis.htm and (Shackley et al. 2016, 2019). Trace element data exhibited here are reported in weight percent (%) and parts per million (ppm), both a quantitative measure by weight as noted.

Santiago Peak Volcanics

A large majority of flaked stone artifacts in western San Diego County sites were produced from rhyolite procured from the Cenozoic Santiago Peak volcanics, as seen in this collection (Herzig and Kimbrough 2014; Jahns and Lance 1950; Tanaka et al. 1984). These are high silica partly metamorphosed (alkali feldspar to quartz) rhyolites that are an excellent raw material particularly for projectile point production, and in many western San Diego County Late Prehistoric sites comprise over 50% of the raw material. The brittleness of the material is such that fine serration and keyhole notching is possible, and I would rate it as midway between a chert and obsidian as a knapping raw material. Prehistoric knappers in the region may have classified these rocks differently (Hohenthal 1950). The rhyolite of Santiago Peak volcanics outcrops throughout southwestern San Diego County, particularly on Dictionary Hill, and in boulders in the middle Sweetwater River Valley near the current Sweetwater Reservoir (see Shackley 2017; Tanaka et al. 1984, Figure 1; Figure 1 here).

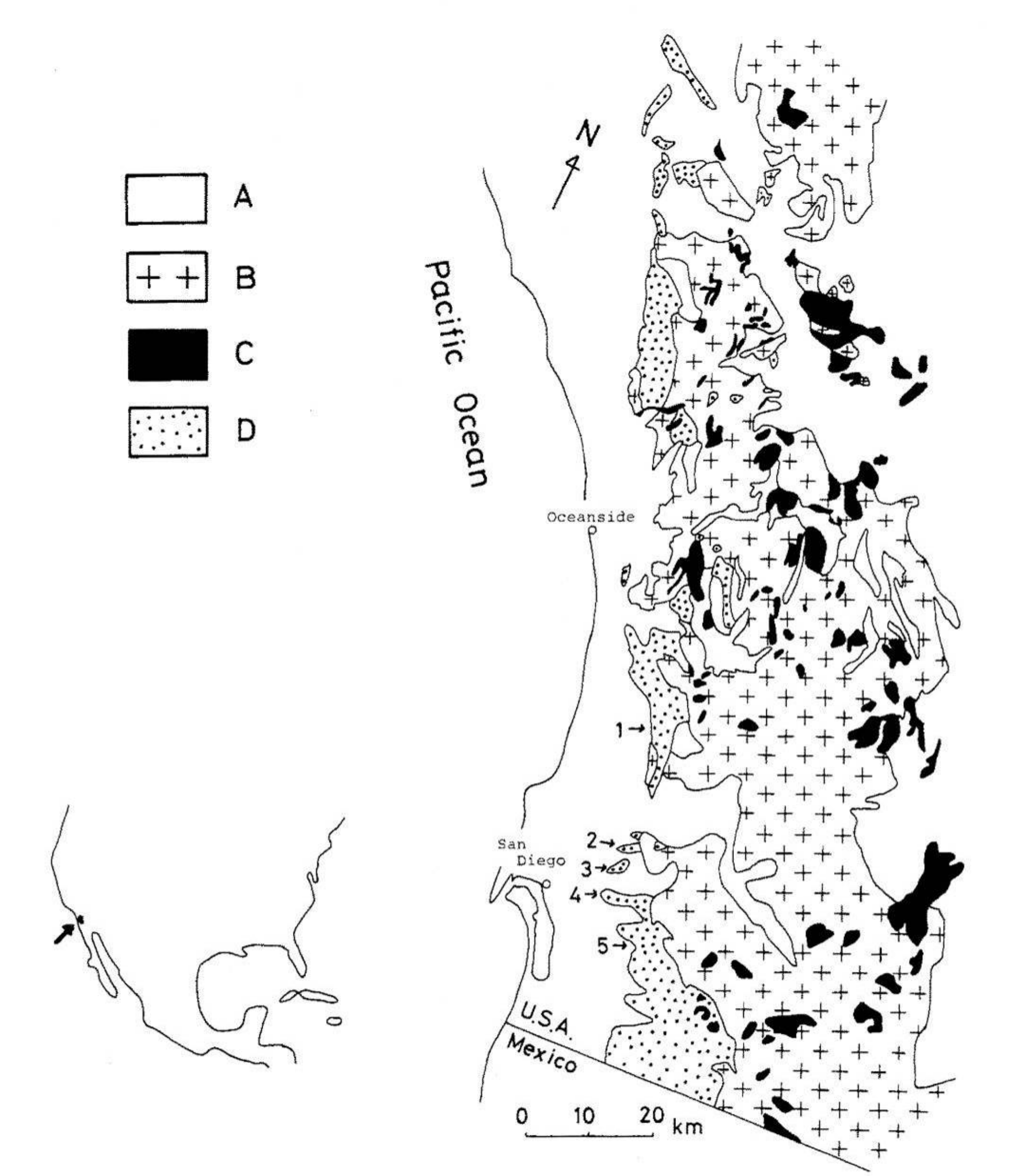

FIG. 1 – Locality index and generalized geological map of the western Peninsular Ranges in southern California.
A: Sediments; B: Granitic rocks; C: Gabbroic rocks; D: The Santiago Peak Volcanic Rocks; 1: The Black Mountain area; 2: The Mission Gorge area; 3: The Murray Reservoir area; 4: The La Mesa area; 5: The Sweetwater Reservoir area. The distribution area of the Santiago Peak Volcanics is compiled from LARSEN (1948), WEBER (1963) and KENNEDY and PETERSON (1975).

Figure 1. Location of Santiago Peak volcanics in San Diego County from Tanaka et al (1984:154). Locations 4 (La Mesa/Dictionary Hill) and 5 (Sweetwater Reservoir) areas where high silica rhyolite occurs, similar to the analyzed samples in this study (see also Herzig and Kimbrough 2014).

Santiago Peak Volcanics consist of basalt, andesite, and rhyolite dated by $^{40}Ar/^{39}Ar$ between 128-117 Ma and predate the Peninsular Range batholith uplift (granitoids and gabbros) by at least 1 Ma (Herzig and Kimbrough 2014). Tanaka et al. (1984:156, Tables 1 and 2) analyzed, by WXRF, a number of samples from Santiago Peak volcanics from western San Diego County, including samples from a dome in his La Mesa area, possibly Dictionary Hill, and domes and outcrops in the Sweetwater Reservoir area of the middle Sweetwater River Valley. These high silica rhyolites are compositionally similar to the two samples analyzed from CA-SDI-4520 (Matamó) in the middle Sweetwater River Valley (Table 2 and Figures 4 and 5; Shackley 2017). That analysis indicated that the artifacts were produced from high silica rhyolites with a composition remarkably similar to those source samples collected by Tanaka et al. (1984), and different in trace element chemistry from the Lusardi Formation samples (Figure 5). Since these rhyolites are so common in western San Diego County, it is likely that most of the Santiago Peak rhyolite raw material used by Late Prehistoric knappers in this part of the county was from these or closely compositionally related sources (Heizer and Treganza 1944). A thorough raw material study could buoy this assumption.

Lusardi Formation SPV Results

The analysis of the Lusardi Formation rocks followed the same protocol as the SDI-4520 samples (Shackley 2017). There are general compositional differences between the three project samples (Lusardi, SDI-4520, and Tanaka), and Tanaka's analyses suggest, as mentioned, that the Sweetwater Reservoir samples are more similar to the SDI-4520 artifacts (see Tables 1 and 2 and Figures 4 and 5). Further collection and analysis of SPV rocks, particularly in southwestern San Diego County (i.e. Dictionary Hill and the Mount Miguel/Sweetwater area) will likely prove fruitful.

With regard to the Lusardi Formation composition, again they are dominated by a rhyolite composition based on the TAS plots (Table 1 and Figure 1). There does not seem to be an issue with patination of the cortical rocks versus freshly broken surfaces since all the rocks patinated or freshly broken cluster relatively closely in both major and trace element plots with the exception of samples 7, 12, and 16 (Figures 4 and 5).

A comprehensive field and laboratory analytical study of the Santiago Peak Volcanics in San Diego County seems warranted similar to the northern New Mexico dacite study (Shackley 2011b). As one of the major toolstones in prehistoric contexts in the region it is certainly needed (see Pigniolo 1996). The SPV rocks in the southern portion of the Santiago Peak Volcanics seem at this juncture to be more aphyric and better suited to chipped stone tool production, but since there has as yet been so little research on the subject, this remains inferential.

REFERENCES CITED

Davis, M.K., T.L. Jackson, M.S. Shackley, T. Teague, and J. Hampel, 2011, Factors Affecting the Energy-Dispersive X-Ray Fluorescence (EDXRF) Analysis of Archaeological Obsidian. In *X-Ray Fluorescence Spectrometry (XRF) in Geoarchaeology*, edited by M.S. Shackley, pp. 45-64. Springer, New York.

Govindaraju, K., 1994, 1994 Compilation of Working Values and Sample Description for 383 Geostandards. *Geostandards Newsletter* 18 (special issue).

Hampel, Joachim H., 1984, Technical Considerations in X-ray Fluorescence Analysis of Obsidian. In *Obsidian Studies in the Great Basin*, edited by R.E. Hughes, pp. 21-25. Contributions of the University of California Archaeological Research Facility 45. Berkeley.

Heizer, R.F. and A.E. Treganza, 1944. Mines and quarries of the Indians of California. *California Journal of Mines and Geology* 40:291-359.

Herzig, C.T., and D.L. Kimbrough, 2014, *Santiago Peak volcanics: Early Cretaceous arc volcanism of the western Peninsular Ranges batholith, southern California.* The Geological Society of America Memoir 211.

Hildreth, W., 1981, Gradients in Silicic Magma Chambers: Implications for Lithospheric Magmatism. *Journal of Geophysical Research* 86:10153-10192.

Hohenthal, W.D., Jr. 1950, *Southern Diegueño Use and Knowledge of Lithic Materials.* Kroeber Anthropological Papers 2. University of California, Berkeley.

Hughes, Richard E., and Robert L. Smith, 1993, Archaeology, Geology, and Geochemistry in Obsidian Provenance Studies. *In Scale on Archaeological and Geoscientific Perspectives*, edited by J.K. Stein and A.R. Linse, pp. 79-91. Geological Society of America Special Paper 283.

Jahns, R.H., and J.F. Lance, 1950, *Geology of the San Dieguito Pyrophyllite Area, San Diego County, California*. Special Report 4, Divsion of Mines, Department of Natural Resources, San Francisco.

Le Maitre, R.; Bateman, P.; Dudek, A.; Keller, J.; Lameyre, J.; Le Bas, M.; Sabine, P.; Schmid, R.; Sorensen, H.; Streckeisen, A.; Woolley, A.; Zanettin, B. 1989, A classification of igneous rocks and glossary of terms: recommendations of the International Union of Geological Sciences Subcommission on the Systematics of igneous rocks (Le Maitre, R.W.; editor). Blackwell*,* 193 p. Oxford.

Lundblad, S.P., P.R. Mills, A. Drake-Raue, and S.K. Kikiloi, 2011, Non-destructive EDXRF analyses of archaeological basalts. In *In M.S. Shackley (Ed.) X-Ray Fluorescence Spectrometry (XRF) in Geoarchaeology*, pp. 65-80. Springer Publishing, New York.

Mahood, Gail A., and James A. Stimac, 1990, Trace-Element Partitioning in Pantellerites and Trachytes. *Geochemica et Cosmochimica Acta* 54:2257-2276.

McCarthy, J.J., and F.H. Schamber, 1981, Least-Squares Fit with Digital Filter: A Status Report. In *Energy Dispersive X-ray Spectrometry*, edited by K.F.J. Heinrich, D.E. Newbury, R.L. Myklebust, and C.E. Fiori, pp. 273-296. National Bureau of Standards Special Publication 604, Washington, D.C.

Pigniolo, A. R. 1996, Lithic material types as a chronological indicator in the archaeological record of San Diego County. In *Proceedings of the Society for California Archaeology, Volume 9*. Judyth Reed, (Ed.). Society for California Archaeology.

Schamber, F.H., 1977, A Modification of the Linear Least-Squares Fitting Method which Provides Continuum Suppression. In *X-ray Fluorescence Analysis of Environmental Samples*, edited by T.G. Dzubay, pp. 241-257. Ann Arbor Science Publishers.

Shackley, M.S., 1988, Sources of archaeological obsidian in the southwest: an archaeological, petrological, and geochemical study. *American Antiquity* 53:752-772.

Shackley, M. S.,1995, Sources of archaeological obsidian in the greater american southwest: an update and quantitative analysis. *American Antiquity* 60(3):531-551.

Shackley, M.S., 2005, *Obsidian: Geology and Archaeology in the North American Southwest*. Tucson: University of Arizona Press.

Shackley, M.S., 2011a, An Introduction to X-Ray Fluorescence (XRF) Analysis in Archaeology. In *X-Ray Fluorescence Spectrometry (XRF) in Geoarchaeology*, M.S. Shackley (Ed.), pp. 7-44. Springer, New York.

Shackley, M.S., 2011b, Sources of archaeological dacite in northern New Mexico. *Journal of Archaeological Science* 38:1001-1007.

Shackley, M.S., F. Goff, and S.G. Dolan, 2016, Geologic origin of the source of Bearhead Rhyolite (Paliza Canyon) obsidian, Jemez Mountains, northern New Mexico. *New Mexico Geology* 38:52-62.

Shackley, M.S., L.E. Morgan, and D. Pyle, 2018, Elemental, isotopic, and geochronological variability in Mogollon-Datil Volcanic Province archaeological obsidian, southwestern North America: solving issues of inter-source discrimination. *Geoarchaeology* 33:486-497.

Tanaka, H., T.E. Smith, and C.H. Huang, 1984, The Santiago Peak volcanic rocks of the Peninsular Range batholith, Southern California: volcanic rocks associated with coeval gabbro. *Bulletin of Volcanology* 47:153-171.

Table 1. Major and minor oxide values for the Lusardi Formation volcanic rock source standards, and USGS RGM-1 rhyolite standard. All measurements in percent by weight or parts per million, as noted[1].

Sample	Na2O	MgO	Al2O3	SiO2	P2O5	K2O	CaO	TiO2	V2O5	Cr2O3	MnO	Fe2O3	Σ
	%	%	%	%	%	%	%	%	%	%	%	%	
1	5.67	0.00	15.283	74.25	0	1.63	1.13	0.45	0.008	0.001	0.034	1.39	99.85
2	2.85	0.10	9.541	79.41	0	3.77	1.48	0.22	0	0	0.025	2.28	99.67
3	3.99	0.00	9.97	80.69	0	2.87	0.60	0.16	0	0.001	0.015	1.57	99.87
4	3.15	0.47	12.826	77.08	0	3.24	1.09	0.22	0	0.006	0.013	1.65	99.74
5	3.50	0.00	11.656	78.06	0	4.26	0.40	0.19	0.012	0.005	0.018	1.68	99.78
6	3.75	0.41	13.648	76.50	0	3.10	1.01	0.13	0.002	0	0.017	1.26	99.83
7	2.04	2.59	16.247	70.94	0	3.77	1.27	0.40	0.037	0.004	0.039	2.40	99.75
8	4.50	0.00	14.488	76.41	0	2.68	0.76	0.15	0.003	0	0.009	0.87	99.87
9	4.29	0.15	14.528	74.49	0	3.55	0.69	0.17	0.016	0	0.022	1.93	99.82
10	3.57	0.15	14.181	75.50	0	3.82	0.53	0.20	0.003	0	0.022	1.84	99.80
11	4.82	0.00	14.48	72.88	0	4.87	0.75	0.14	0.001	0.003	0.021	1.87	99.84
12	4.31	0.00	19.37	68.49	0	4.40	1.26	0.19	0.011	0.002	0.046	1.75	99.82
13	5.48	0.00	14.332	73.93	0	2.89	1.13	0.19	0.015	0.002	0.019	1.87	99.87
14	2.48	1.02	13.533	77.74	0	3.32	0.80	0.14	0.017	0	0.012	0.70	99.78
15	3.25	0.41	13.18	76.09	0	3.20	1.18	0.24	0.011	0.002	0.026	2.24	99.81
16	5.63	0.00	12.419	77.80	0	0.06	0.85	0.38	0.018	0.007	0.032	2.75	99.94
RGM1-S4	3.93	0.00	13.144	73.76	0	4.93	1.43	0.31	0	0	0.046	2.22	99.77
Sample	Cl	Ni	Cu	Zn	Ga	Rb	Sr	Y	Zr	Nb	Ba	Pb	Th
	ppm	ppm	ppm	ppm	ppm	ppm	ppm	ppm	ppm	ppm	ppm	ppm	ppm
1	73.129	16	4	19	16	47	81	39	181	4	904	10	12
2	610.06	17	10	40	14	102	91	35	157	8	1286	9	8
3	0	15	5	16	12	50	76	24	120	5	1034	5	4
4	387.051	16	4	27	12	72	90	29	164	2	1111	9	12
5	0	14	0	33	13	102	86	28	196	5	1301	7	17
6	0	14	4	22	17	76	94	25	175	7	954	6	8
7	255.983	16	11	54	19	110	117	23	188	4	1277	11	21
8	0	16	4	29	15	59	79	23	177	5	759	8	13
9	0	14	3	26	16	86	95	30	168	2	969	13	5
10	0	16	9	32	15	94	100	39	177	11	1161	13	8

Sample	Cl	Ni	Cu	Zn	Ga	Rb	Sr	Y	Zr	Nb	Ba	Pb	Th
11	0	15	3	16	14	75	82	29	188	6	977	4	12
12	0	16	1	33	16	83	108	24	171	2	1001	9	18
13	0	16	0	25	15	55	97	16	190	2	905	3	5
14	0	15	3	58	15	77	106	19	159	1	1163	18	5
15	0	15	2	30	17	76	99	21	165	4	980	9	12
16	0	16	2	19	15	0	78	18	285	6	60	3	9
RGM1-S4	439.715	15	13	43	16	145	106	28	225	10	802	19	19

[1] H_2O and LOI not calculated here.

Table 2. XRF analysis of black and green Santiago Peak Volcanic specimens from CA-SDI-4520 (Matamó), middle Sweetwater River Valley, San Diego County, California (see Figure 2, 3 and 5; Shackley 2017). The major, minor, and trace element data are very similar to that analyzed by Tanaka et al. (1984) from Sweetwater Reservoir just downstream from CA-SDI-4520. Compare to the Lusardi Formation SPV composition in Table 1.

Sample	Na2O	MgO	Al2O3	SiO2	P2O5	Cl	K2O	CaO	TiO2	V2O5	Cr2O3	MnO	Fe2O3
	%	%	%	%	%	ppm	%	%	%	%	%	%	%
POINT2 GREEN	2.13	0.66	10.87	75.90	0	1862.73	1.26	4.24	0.32	0.02	0	0.08	4.2
POINT3 BLACK	3.46	1.10	12.46	72.08	0	1963.76	1.46	2.07	0.50	0.01	0.002	0.14	6.40
	Ni	Cu	Zn	Rb	Sr	Y	Zr	Nb	Ba	Pb	Th		
	ppm	ppm	ppm	ppm	ppm	ppm	ppm	ppm	ppm	ppm	ppm		
POINT2 GREEN	17	12	81	37	131	47	205	3	684	1	4		
POINT3 BLACK	21	24	156	42	103	51	248	9	483	15	5		

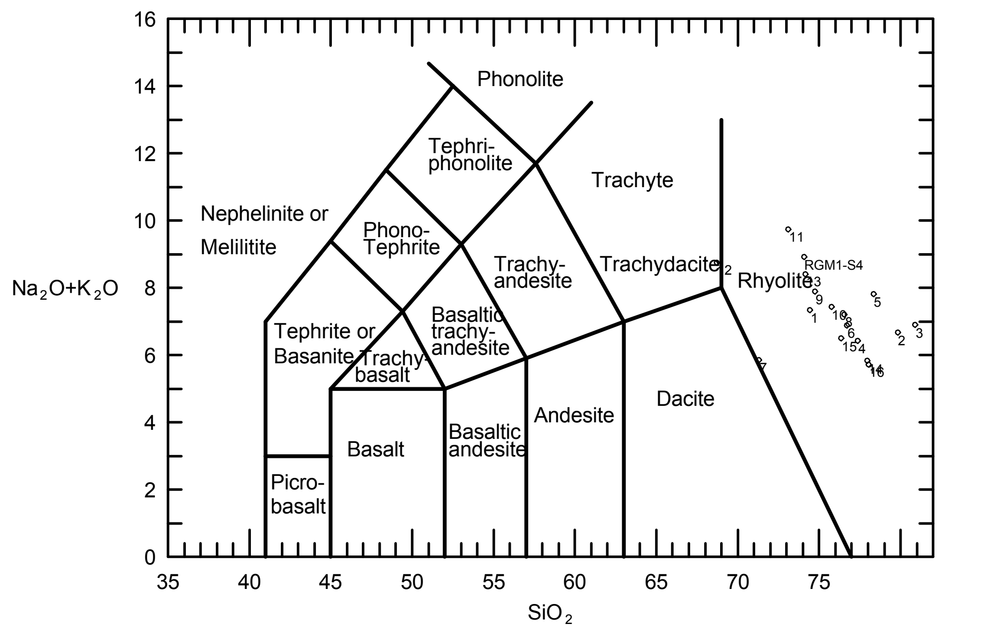

Figure 1. TAS plot of the Lusardi Formation rock samples and RGM-1 (Le Maitre et al. 1989).

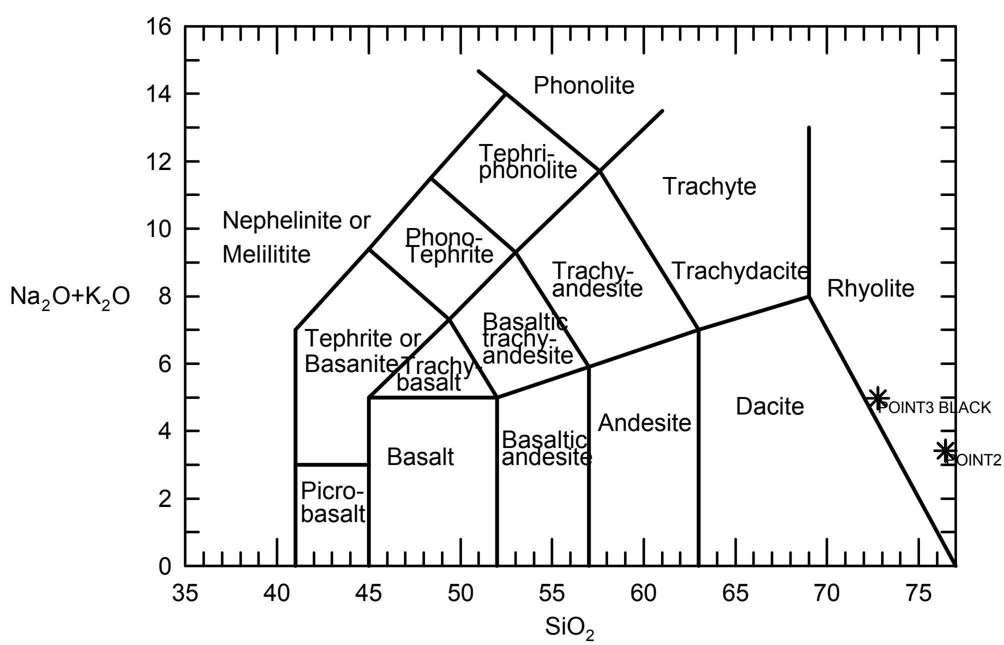

Figure 2. TAS plot of two Santiago Peak Volcanic artifacts from SDI-4520 (LeMaitre et al.1989).

Figure 3. The two projectile point preforms of Santiago Peak volcanic raw materials analyzed by XRF from SDI-4520 (Table 2). The black sample on left and the gray-green sample on right.

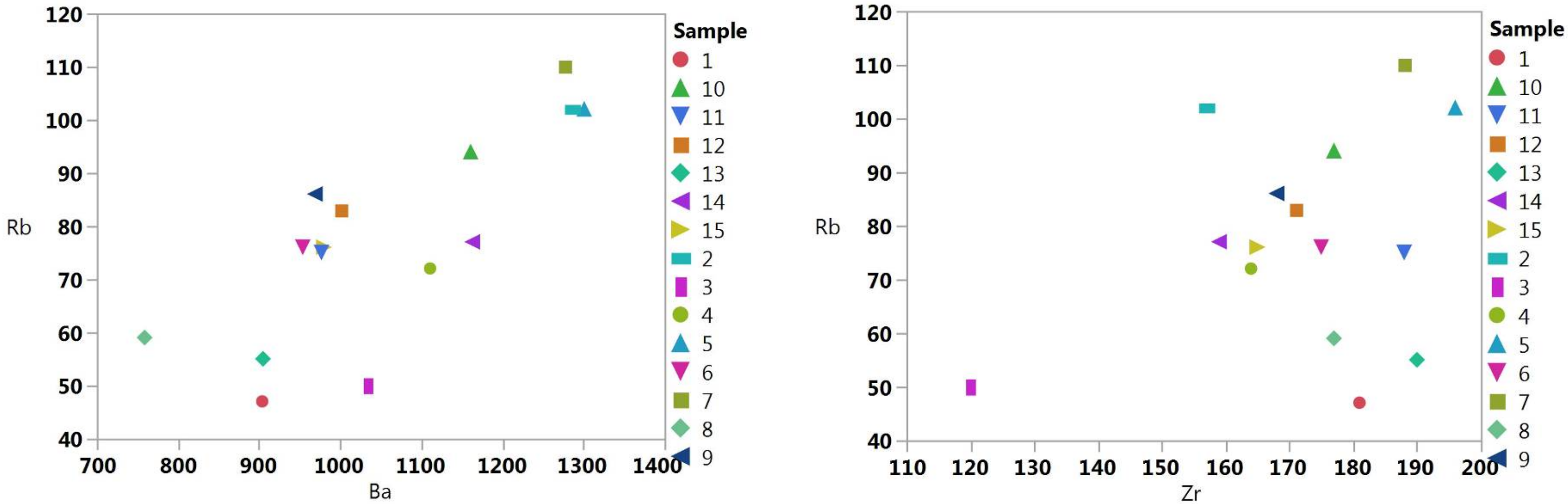

Figure 4. Ba/Rb and Zr/Rb bivariate plots of the Lusardi Formation samples. Sample 16 not included.

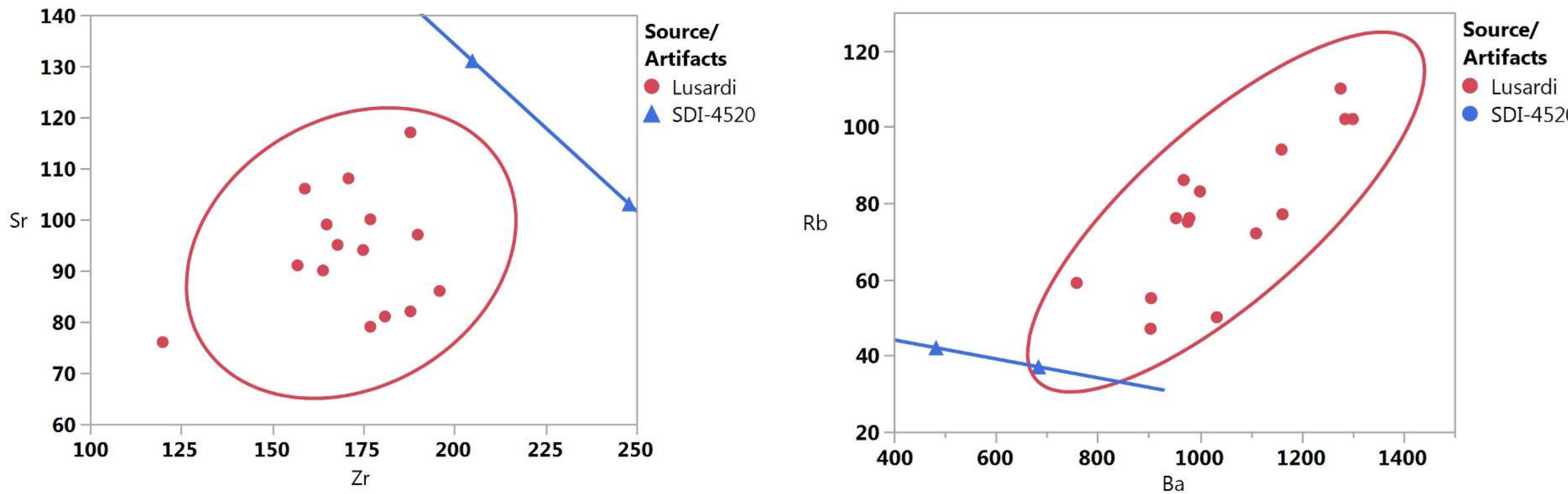

Figure 5. Zr/Sr and Ba/Rb bivariate plots of the Lusardi Formation source samples and the two SPV rhyolite artifacts from SDI-4520. Confidence ellipses at 95%.